Zeitschrift: IABSE congress report = Rapport du congrès AIPC = IVBH

Kongressbericht

Band: 3 (1948)

Artikel: Performance of thin steel compression flanges

Autor: Winter, George

DOI: https://doi.org/10.5169/seals-4005

Nutzungsbedingungen

Die ETH-Bibliothek ist die Anbieterin der digitalisierten Zeitschriften auf E-Periodica. Sie besitzt keine Urheberrechte an den Zeitschriften und ist nicht verantwortlich für deren Inhalte. Die Rechte liegen in der Regel bei den Herausgebern beziehungsweise den externen Rechteinhabern. Das Veröffentlichen von Bildern in Print- und Online-Publikationen sowie auf Social Media-Kanälen oder Webseiten ist nur mit vorheriger Genehmigung der Rechteinhaber erlaubt. Mehr erfahren

Conditions d'utilisation

L'ETH Library est le fournisseur des revues numérisées. Elle ne détient aucun droit d'auteur sur les revues et n'est pas responsable de leur contenu. En règle générale, les droits sont détenus par les éditeurs ou les détenteurs de droits externes. La reproduction d'images dans des publications imprimées ou en ligne ainsi que sur des canaux de médias sociaux ou des sites web n'est autorisée qu'avec l'accord préalable des détenteurs des droits. En savoir plus

Terms of use

The ETH Library is the provider of the digitised journals. It does not own any copyrights to the journals and is not responsible for their content. The rights usually lie with the publishers or the external rights holders. Publishing images in print and online publications, as well as on social media channels or websites, is only permitted with the prior consent of the rights holders. Find out more

Download PDF: 16.10.2025

ETH-Bibliothek Zürich, E-Periodica, https://www.e-periodica.ch

Le comportement des éléments comprimés de faible épaisseur

Das Verhalten dünnwandiger Druckgurte

Performance of thin steel compression flanges

D' GEORGE WINTER

Professor of Structural Engineering, Cornell University, Ithaca, N. Y., U. S. A.

The economic use of standard, hot-rolled steel shapes is limited to relatively substantial structures. The need for lighter steel members for small scale industrial, commercial and residence building initiated the use of structural members made from sheet steels by cold forming (cold rolling or pressing). Roof decks of a considerable variety of sizes and shapes, formed in this manner, as well as structural shapes of I-, channel, and similar sections, have been in use in the U. S. A. for many years. The development of automatic spot welding on the one hand, and the wartime demand for light, pre-fabricated buildings on the other, have stimulated this development.

It was soon realized, however, that accepted design procedures had to be modified to suit the special requirements of such thin-walled structures. The American Iron and Steel Institute, in 1939, inaugurated a research program under the writer's direction at Cornell University, which has resulted in the « Specifications for the Design of Light Gage Steel Structural Members » issued by the Institute in 1946.

One of the main problems in this connection is that of the performance of thin compression plates, both at loads causing failure and at the lower design loads. In this connection two types of such plates must be distinguished:

- a) Long plates that are stiffened along both longitudinal edges, such as webs of channels and I-beams;
- b) Long plates that are stiffened only along one longitudinal edge, such as the flanges of channels, I-sections, and angles.

The present paper is concerned only with the first of these two types. The classical theory of elasticity allows the calculation of critical buckling loads of such plates by the so-called small deflection theory, that is by the solution of the differential equation

$$\frac{\partial^4 w}{\partial x^4} + 2 \frac{\partial^4 w}{\partial x^2 \partial y^2} + \frac{\partial^4 w}{\partial y^4} = -\frac{st}{D} \frac{\partial^2 w}{\partial x^2}. \tag{1}$$

In contrast to the phenomenon of column buckling, the critical stresses calculated from eq. 1 do not represent the limit of carrying capacity of edge supported plates. Indeed, in such plates, deflections can not increase indefinitely, as they do in columns at the Euler load. Consequently, once the critical stress is passed, the hitherto plane plate merely deforms into a non-developable, wavy surface, but continues to resist increasing stress. The deformations just described result in additional, particularly transverse stresses which act jointly with the imposed, primary longitudinal compression stress. In analyzing this state one can no longer neglect the influence of the deflections on the distribution of stress, which had been the basis for the development of eq. 1.

The differential equation for this large deflection buckling of plates

was developed by Th. v. Kármán in 1910, and reads as follows

$$\frac{\partial^{4} w}{\partial x^{4}} + 2 \frac{\partial^{4} w}{\partial x^{2} \partial y^{2}} + \frac{\partial^{4} w}{\partial y^{4}}$$

$$= \frac{t}{D} \left(\frac{\partial^{2} F}{\partial y^{2}} \frac{\partial^{2} w}{\partial x^{2}} - 2 \frac{\partial^{2} F}{\partial x \partial y} \frac{\partial^{2} w}{\partial x \partial y} + \frac{\hat{o}^{2} F}{\partial x^{2}} \frac{\partial^{2} w}{\partial y^{2}} \right) \tag{2}$$

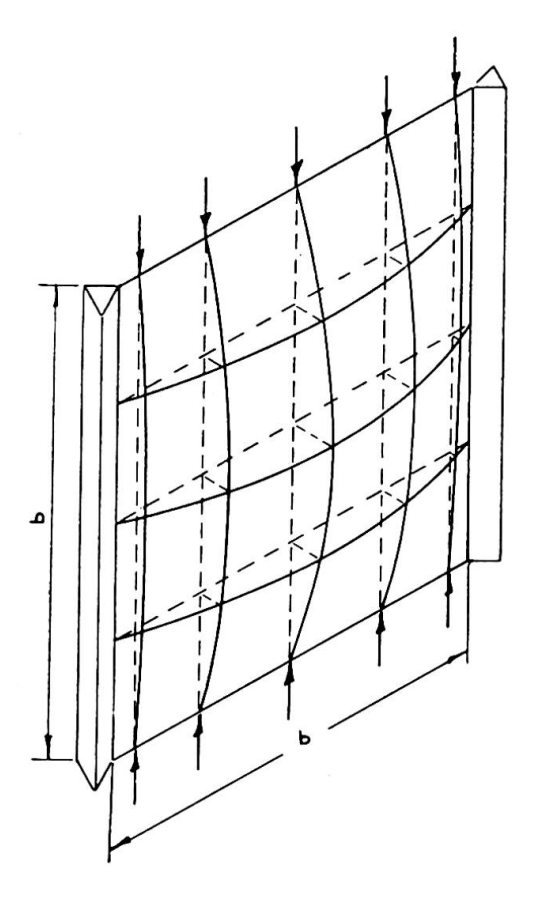
where F is a stress function. The complexity of this equation has so far prevented its explicit solution for rectangular plates. It is for this reason that this problem had to be investigated primarily by experimental methods.

In this connection the concept of the equivalent width, initiated by Th. v. Kármán, proved most helpful. This concept is best visualized by means of a model. Imagine a square compressed plate replaced by a lattice of bars. Beyond the buckling load of the compressed rods the lattice will obviously distort in the manner shown in fig. 1. Two circumstances are

clear from this picture:

a) The compression bars cannot fail as simple columns by continued deflection because they are restrained from doing so by the cross-bars.

b) In the stage shown in the figure the total load is obviously not equally distributed among the compression bars; in view of the variations of the deflections the bars near or at the edges carry more load than those near



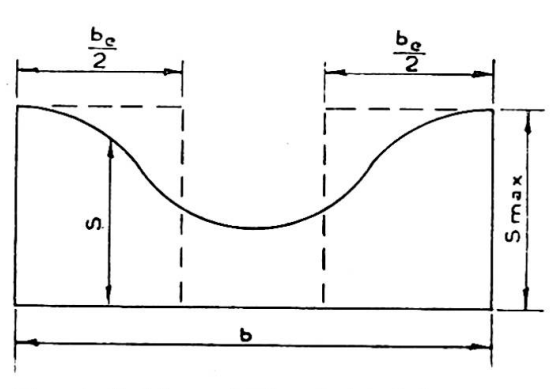


Fig. 1 (left) and Fig. 2 (right).

the center, and failure will occur when the more heavily loaded bars

will reach their yield strength.

It can be seen, therefore, that after first buckling has occurred, the stress in a compressed plate must show a distribution as given in fig. 2. The effective width b_e is that width which will make the area under the dotted lines equal to the area under the actual solid stress curve. Once this effective width is determined, design can proceed in the usual manner, merely by replacing the actual plate area $b \times t$ by the equivalent area $b_e \times \check{t}$. T. v. Kármán gave the following tentative expression for this effective width at the failure load:

$$b_{c} = \frac{\pi}{\sqrt{3(1-v^{2})}} t \sqrt{\frac{E}{s_{yp}}} = 1.9 t \sqrt{\frac{E}{s_{yp}}}$$
 (3)

for Poisson's ratio $\gamma = 0.3$ (1).

Subsequent tests by E. E. Sechler showed that this expression was reasonably correct for very wide and thin plates, but that a smaller value of b_e results for plates of smaller b/t-values (2).

All these investigations were concerned only with the determination of the ultimate or yield strength of such plates. In addition, the amount

of test evidence even in this respect was limited.

For practical design, however, it is necessary to determine equivalent widths not only at failure, but also at smaller loads, in particular at service loads. Indeed, since slight buckling occurs for large b/\bar{t} at loads far below the ultimate, the stress distribution of the type of fig. 2 takes place not only at failure but frequently at design loads. Hence, in a flexual member of the type of fig. 3, stresses and corresponding deformations are distributed at design loads in the manner shown. The neutral axis of such a member is then located below the centroid of the area, and its location as well as the moment of inertia, section modulus, etc. must be computed by using the equivalent instead of the real width of the compression flange. That is, in order to compute stresses, deflections, and other design information for any load up to failure, the actual section, fig. 3a, with its non-uniform stress distribution can be replaced by the equivalent section, fig. 3b. Since the maximum stresses, and corresponding strains, at the edges of the webs are equal for these two sections, all required information can be gained from this equivalent section.

It was therefore necessary for practical design to determine the effec-

tive width not only at failure, but also at lower loads.

For this purpose more than 100 tests were carried out on members of the type of fig. 3, and other shapes, with b/t-ratios from 14 to 429 and with steel yield points from 20 100 to 57 800 psi. Deformations were measured in these flexural tests and it was found, as anticipated, that the neutral axis was located below the centroid, and was shifting downward under increasing load, i.e. with decreasing effective width.

Only the most recent of these tests are reported here (3).

Specimens of these tests were of the type of fig. 3a, 3 in deep, 5 to 10 in wide, with thicknesses from 0.0288 tot 0.0615 in. Corresponding width/

⁽¹⁾ Th. v. Kármán, E. E. Seguler, L. H. Donnell, The Strength of Thin Plates in Compression (Trans. Am. Soc. Mech. Eng., Vol. 54, 1932, p. 53).
(2) E. E. Seguler, The Ultimate Strength of Thin Flat Sheet in Compression, Publication No. 27, Guggenheim Aeronautics Labor, Pasadena, Cal., 1933.
(3) Geo. Winter, The Strength of Thin Steel Compression Flanges (Proc. Am. Soc. Civ. Eng.,

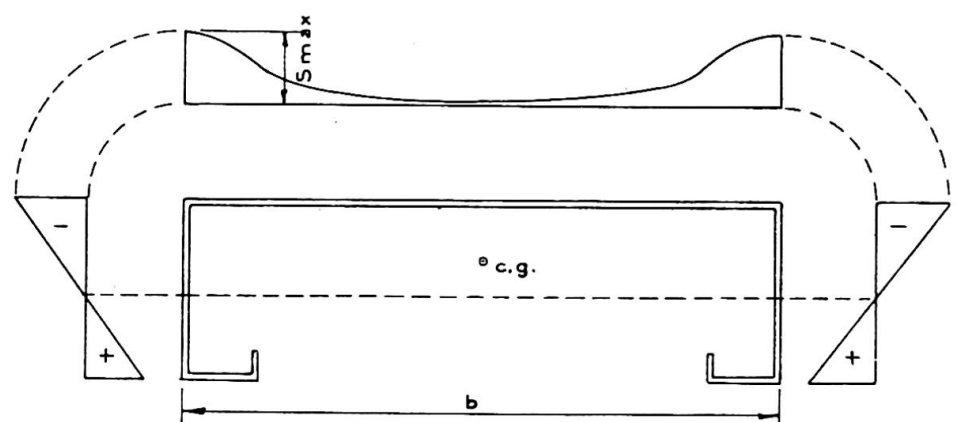


Fig. 3a.

thickness ratios b/t ranged from 86 to 344, yield points of steels, from tension tests, were found to range from 24 400 to 56 850 psi. Specimens were tested as beams, with two equal loads at the quarter points of the span. In addition to deflections, strains were measured at the top and bottom of the flanges, allowing an experimental determination of the position of the neutral axis. Finally, displacements of the top flange out of its original plane were measured at six points along the center line, in the portions of the beams between loads.

Information on the magnitude of the equivalent width was gained from these tests in the following manner: The position of the neutral axis, at various loads, was established from strain gage readings. Knowing this position, in a section like fig. 3b, it is simple to compute the corresponding value of b_c . With the equivalent section determined in this manner, the maximum compression stress s_{\max} corresponding to the particular load is computed by customary methods. The tests, therefore, give information on the relation of b_c to b/t and s_{\max} .

To evaluate this relation, eq. 3 is rewritten as

$$b_c = Ct \sqrt{\frac{\overline{E}}{s_{\text{max}}}} \tag{4}$$

where C is a coefficient to be determined from test. Previous investigations by Sechler and the writer (2) (3) established that C depends primarily on

the non-dimensional parameter $\sqrt{\frac{E}{s_{\text{max}}}} \left(\frac{t}{b}\right)$. It is for this reason that,

in fig. 4, the experimentally determined coefficients C are plotted against this parameter. Determinations were made, for each test specimen, at the yield load and at 1/3 and 2/3 of that load.

Although the scattering of test results, as depicted in fig. 4, is quite considerable it is clearly seen that the coefficient C decreases with increasing

 $\sqrt{\frac{E}{s_{\max}}}\left(\frac{t}{b}\right)$. The scattering is apparently due to the extreme sensitivity of this method to very minor experimental deviations. Indeed, a variation of 1 % in the experimentally determined location of the neutral axis will cause, in many cases, a variation of 10 % and more of the value of C. For

Vol. 72 p. 199, 1946 and Trans. Am. Soc. Civ. Eng., Vol. 112, p. 1, 1947). See also Bull. No. 35, Part 3, Cornell University Engg. Experiment Station, Ithaca, N. Y., 1947.

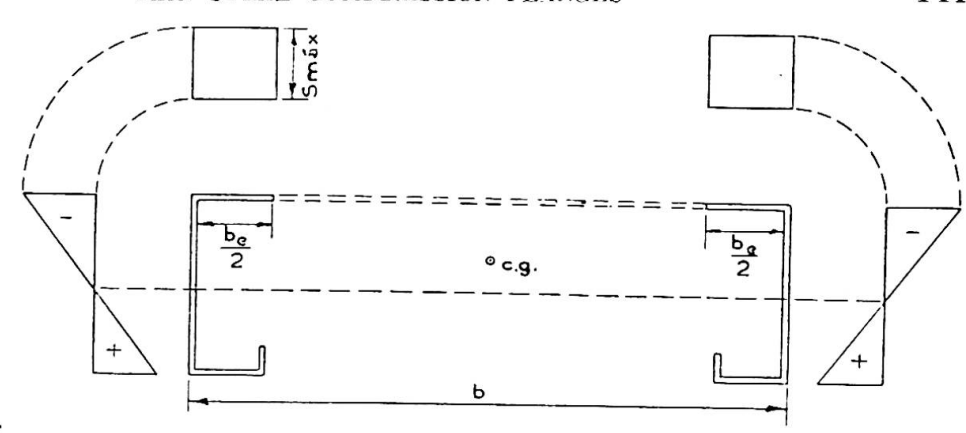


Fig. 3b.

this reason, in interpreting fig. 4, the data should be regarded as statis tically distributed, rather than as strictly accurate.

With this in mind, the straight line drawn on that figure was thought to represent a reasonable, and somewhat conservative means of developing a simple formula for the equivalent width b_c . The line is seen to start at a value of 1.9 for extremely large b/t-values and relatively high stresses, for which case, therefore, the experimental determinations are in substantial agreement with v. Kármán's original eq. 3. The formula for b_c obtained from this straight line can be written as

$$b_c = 1.9 t \sqrt{\frac{E}{s_{\text{max}}}} \left(1 - 0.475 \frac{t}{b} \sqrt{\frac{E}{s_{\text{max}}}} \right)$$
 (5)

which is seen to be identical with eq. 3, except for the modifying term in parenthesis, which, as pointed out, approaches 1 closely for large b/t and s_{\max} .

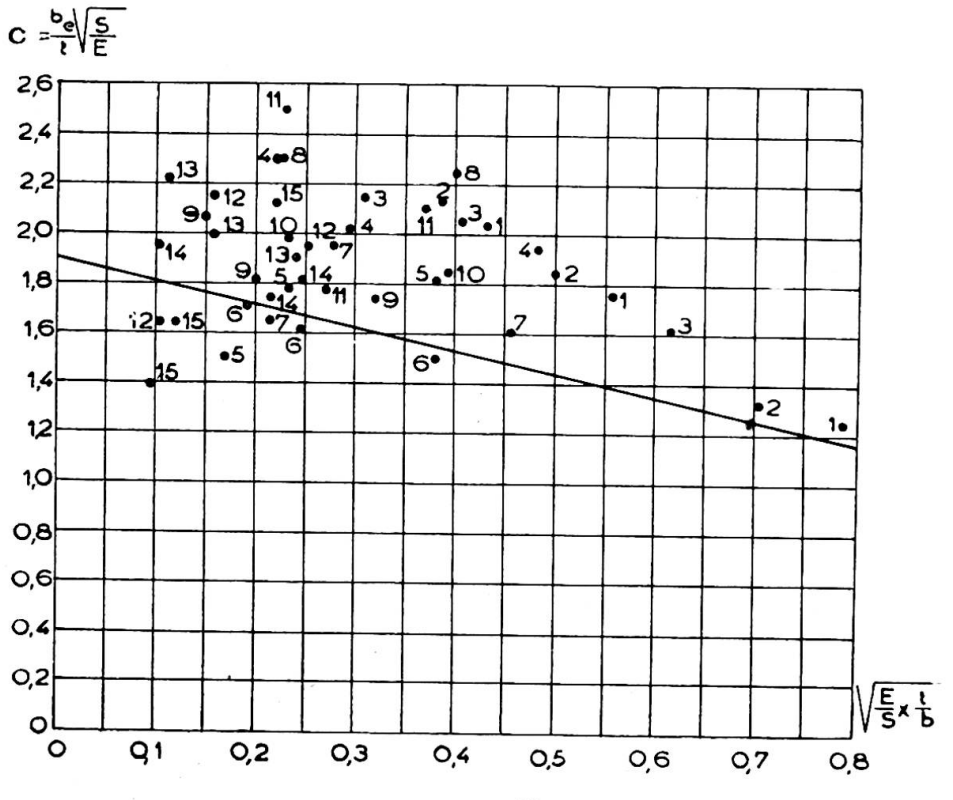


Fig. 4.

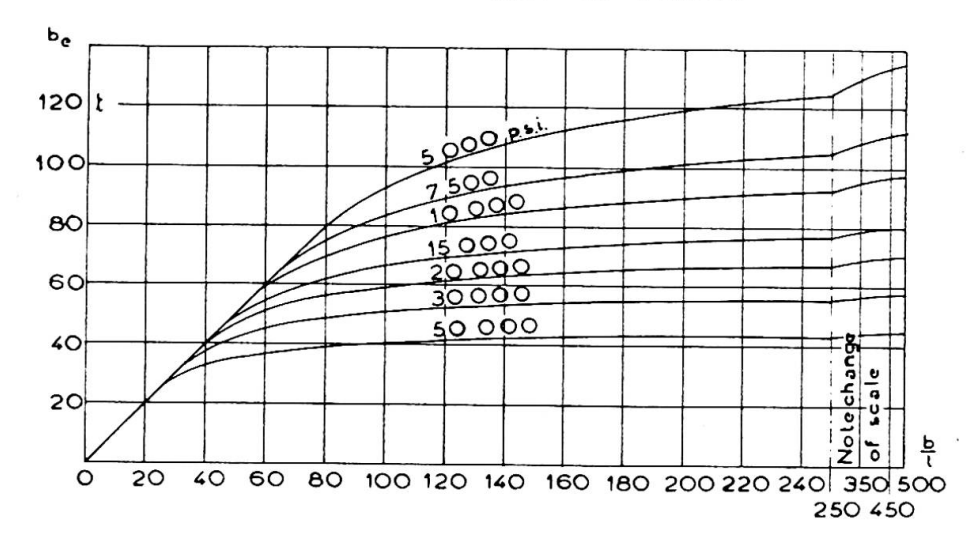


Fig. 5. Effective width of compression elements stiffened along both edges.

Eq. 5 indicates that a compression plate is fully effective (uniform stress distribution, $b_e = b$) for values of b/t smaller than

$$\left(\frac{b}{t}\right)_{L} = 0.95 \sqrt{\frac{E}{s_{\text{max}}}} \tag{6}$$

and that, for values above $(b/t)_{\mathtt{L}}$ deformations, deflections, and yield loads can be calculated with good accuracy by using the effective instead of the real width.

By solving eq. 6, for $s_{\rm max}$, it can easily be calculated that the first redistribution of stress, that is the first gradual formation of buckling waves occurs at stresses equal to $s_{\rm cr}/4$, where $s_{\rm cr}$ is the critical buckling stress obtained from the small deflection theory, i.e. from eq. 1. This result is not amazing. Theoretically, an ideally plane plate should not buckle at stresses below $s_{\rm cr}$. Actual sheet steel members, however, are not perfect but possess initial distortions of shape, which result in small deflections at stresses below $s_{\rm cr}$. The situation is comparable to that of initially bent or eccentric columns, which also deflect below the Euler load.

The fact that the initial shape has a definite influence on the performance of such plates, causes considerable scattering of test results. These are also influenced by the amount of restraint provided by adjoining members, such as the webs in fig. 3. For this reason eq. 5 represents merely a conservative statistical expression of test results.

Fig. 5 shows a graphical representation of eq. 5 from which the effective width can be read directly for any given b/t and E/s_{max} for use in design.

The findings of this primarily experimental investigation merely represent an elaboration of v. Kármán's concept. They improve the accuracy of his original expression, particularly for plates with moderate b/t. In addition, they prove the important additional finding that the same expression, eq. 5, can be applied with good accuracy to stresses occurring at design loads, as well as to failure stresses.

The real worth of an equation of the type of eq. 5 depends, of course, on the degree of accuracy with which it predicts the actual carrying capacities and deflections of test beams. The following table contains, for the 15 beams whose results are plotted on fig. 4, the yield loads as deter-

mined from test, and those computed by means of the equivalent section, fig. 3b, using eq. 5 for determining the equivalent width.

N•	b / <i>t</i>	Yield Point psi	Yield Load, Computed lb	Yield Load Test lb	Deviation %
1	95	27 500	2 660	2 300	- 13.5 - 1.1 - 8.4 + 4.7 + 14.1 + 8.5 + 3.4 - 0.4 - 1.3 - 4.6 - 11.8 - 2.8 + 9.9 - 10.7 + 3.0 average deviate
2	86	36 000	3 640	3 600	
3	109	37 400	2 730	2 500	
4	145	30 150	1 480	1 550	
5	175	25 750	964	1 100	
6	172	24 700	945	1 025	
7	155	25 850	1 160	1 200	
8	175	47 200	4 520	4 500	
9	163	56 850	5 570	5 500	
10	222	21 400	1 845	1 760	
11	216	36 050	2 550	2 250	
12	284	30 650	1 523	1 480	
13	303	25 100	1 165	1 280	
14	339	28 000	1 052	940	
15	344	27 650	1 028	1 060	

It is seen that, for a very wide range of b/t and yield point stress, eq. 5 allows the prediction of the actual carrying capacity with very satisfactory accuracy. The same was found to be true for the numerous earlier tests (3).

It is interesting to note that despite the rather bad scattering of some points on fig. 4, such as points 4, 8, 11 and 15, the predicted and actual carrying capacities of these four beams, as given in the table, are in very satisfactory agreement. This supports the opinion advanced before that the scattering in fig. 4 is due mainly to inevitable inaccuracies in the empirical determination of the neutral axes.

For practical design, deflections are of interest at design loads rather than at yield loads. Since b_{ϵ} depends on the value of s_{\max} , the effective moment of inertia is variable and must be determined for any given load. The « Design Specifications » mentioned in the introductory paragraphs stipulate a factor of safety of 1.85. For this reason, a comparison of measured and computed deflections is given in the table below for loads approximately equal to the computed yield loads divided by 1.85. Further computations, the results of which are omitted here, show that the same general picture as given in this table obtains for other values of loads, up to the yield load. The table gives the deflections d measured in tests at the load P, and the deflections computed for that load (a) by using the equivalent width b_{ϵ} and (b) by using the full unreduced width b.

N.	P lb	d, from test	d, computed using be, in	0/0	d, computed using b	0.0
1 2 3 4 5 6 7 8 9 10 11 12 13 14 15	1 465 2 000 1 495 811 526 514 635 2 500 3 080 1 010 1 395 833 635 574 559	0.090 0.120 0.128 0.108 0.076 0.068 0.078 0.128 0.170 0.072 0.102 0.083 0.061 0.075 0.077	0.091 0.118 0.131 0.097 0.072 0.068 0.075 0.161 0.195 0.083 0.119 0.100 0.074 0.078 0.075	- 1.1 + 1.7 - 2.3 + 10.2 + 5.6 0.0 + 4.0 - 20.5 - 12.8 - 13.3 - 14.2 - 17.0 - 17.6 - 3.9 + 2.7 Average deviation - 5.2 %	0.085 0.111 0.108 0.076 0.055 0.054 0.060 0.122 0.148 0.064 0.089 0.066 0 055 0.052 0.050	+ 5.6 + 8.1 + 18.5 + 42.1 + 38.2 + 25.9 + 30.0 + 4.9 + 12.5 + 14.6 + 25.8 + 10.9 + 44.2 + 54.0 Average deviation + 23.3 %

The table shows that by using the effective width b_c deflections are computed with an average accuracy of about 5 %, whereas the use of the full, unreduced section for this purpose leads to an average error of about 23 %. Though scattering is again considerable, all significant discrepancies in the first case are on the safe side (computed deflections larger than measured values). On the other hand, by using the full, unreduced sectional area, errors on the unsafe side in several cases reach magnitudes of 40-50 %; by this method, for all beams, actual deflections were found to be larger than computed.

It should be said that an accurate computation of deflections by the equivalent width method would involve the use of a moment of inertia, variable along the beam. Indeed, since b_c depends on s_{\max} , the effective moment of inertia increases from a minimum value at the point of maximum moment to a maximum value near the supports. In the table above, however, only the minimum moment of inertia was used. For the present tests this does not lead to too large an error, since M_{\max} is constant over the center half of the span, for quarter point loading. Had a variable moment of inertia been used, all deflections computed by using b_c would have been obtained slightly smaller, to various relative degrees, resulting in a still better average agreement with test results. This method of calculation was not used because in routine design procedures, engineers can hardly be expected to spend the very considerable amount of time necessary for such detailed calculations with variable moment of inertia.

The evidence presented above, which is additionally supported by a great number of other tests previously published elsewhere (3) indicates that the proposed method allows, with reasonable accuracy, the determination of carrying capacities as well as deflections of members containing thin compression flanges. The measure of agreement with test results is not as close as would be obtained on customary, heavy steel structures. This, however, is predicated on the inherent character of thin sheet material with its inevitably larger imperfections as to accuracy of sheet

thickness, of geometrical shape, etc. The discrepancies obtained in these tests are believed to be tolerable practically; they are certainly not larger than these observed in tests of reinforced concrete or timber structural members.

The use of eq. 5 is somewhat cumbersome for routine design computations. The graph of fig. 5 allows the direct determination of b_e for any given stress and b/t-ratio. The initial straight line to which all curves are tangent indicates the range over which the full width b is effective. It is seen that the larger the maximum stress, the smaller is that limiting b/t beyond which the effectiveness of the flange begins to decrease (see eq. 6).

In contrast to conventional, thick-walled steel structures, the crosssections of thin-walled elements distort at loads far below the ultimate, and in most cases at values even below the design loads. The type and magnitude of these deformations is therefore of interest, since an excessive amount of flange distortion would obviously make such members practically objectionable even if their strengths and over-all deflections were

adequate for the purpose.

These distortions of shape, for members of the type of fig. 3, consist of two separate kinds of deformation which superpose to result in the final shape under load. The first, and more obvious, is the simple buckling deformation. Indeed, ultimate stresses and frequently working stresses are considerably above the critical buckling stress as determined from eq. 1. Moreover, it was mentioned in connection with eq. 6 that on the basis of this equation incipient, extremely slight flange distortions apparently occur at stresses of the order of $s_{\rm cr}/4$. Consequently, at stresses of about that magnitude, the compression flange begins to buckle into a series of approximately quadratice buckling waves. That is, the half-wave length is about equal to the flange width b, and the general shape of each of these half-waves is that schematically indicated on fig. 1. This type of deformation, which was observed in all tests of this kind, is of course exactly the one predicted by the mathematical theory of buckling of plates.

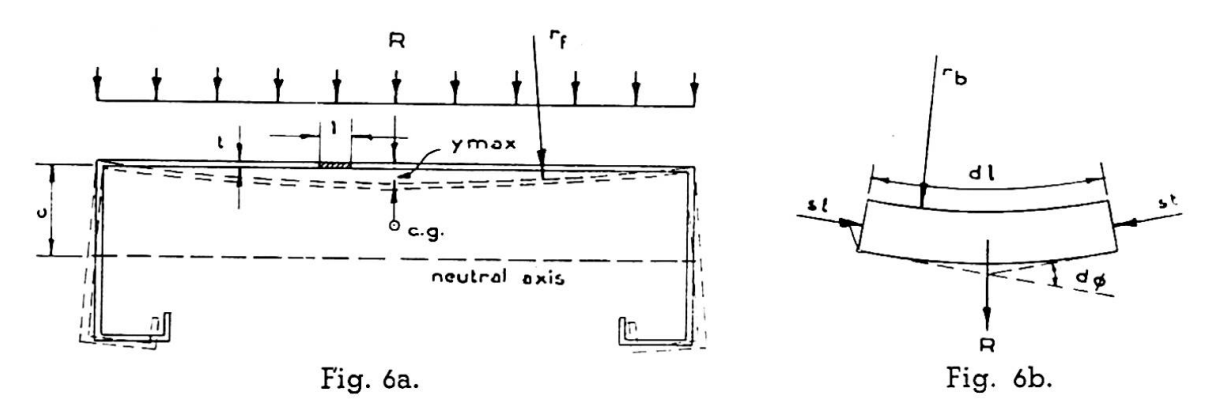
In beam specimens of the type discussed herein, however, a fundamentally different type of deformation is superposed on the one just discussed. This type, which was likewise observed in all tests, is not limited to compression flanges; it occurs likewise if the beams of fig. 3 are turned by 180° so that the wide flange is in tension. The following brief and intentionally approximate analysis illustrates the nature of these deformations and allows a reasonably accurate determination of their magnitude.

Consider an element of the flange, of unit width in the transverse direction, and length dl longitudinally, as shown on fig. 6. Under load, this element is curved, its radius, r_b , being equal to that of the beam at that cross-section. The total compression forces at both ends of the element consequently subtend an angle $d\varphi$ and, therefore have a resultant

$$R = st \frac{d\varphi}{dl} = \frac{st}{r_b} . ag{7}$$

If the stress s is uniform over the width of the cross-section, R acts in the same manner as an external, transverse load, as shown in fig. 6a, tending to bend the flange toward the neutral axis. This bending is governed by the simple equation for flexure of a long, narrow rectangular plate under transverse load, i.e.

$$\frac{d^2y}{dx^2} = -\frac{1}{r_f} = -\frac{M_f}{D}. \tag{8}$$



The maximum deflection is then found from the usual formula

$$\mathbf{y}_{\text{max}} = \frac{5}{384} \frac{st}{r_b} \frac{b^4}{D} . \tag{9}$$

The use of this formula neglects the influence of restraint provided to the flange by the webs. However, this restraint is of rather undetermined magnitude. The webs of isolated beams deform as shown on fig. 6a, and therefore afford little restraint. The restraint would be larger if such beams were laid side by side, with webs in contact, as in a floor. In view of this indeterminacy it seems best to neglect the unreliable effect of possible restraint.

To find r_b for substitution in eq. (9) one has from standard, elementary beam theory

$$r_b = \frac{\mathrm{EI}}{\mathrm{M}_b}; \quad \mathrm{M}_b = \frac{s\mathrm{I}}{c}; \quad r_b = \frac{\mathrm{E}c}{s}.$$
 (10)

With this value of r_b , the maximum flange distortion becomes

$$y_{\text{inax}} = \frac{5}{32} \left(\frac{s}{E} \right)^2 \cdot \frac{b^4}{t^2 c} (1 - y^2) . \tag{11}$$

For tension flanges with their generally rather uniform stress distribution, this type of distortion is the only one that occurs and its magnitude can be determined with satisfactory accuracy from eq. 11. In compression flanges the longitudinal stresses vary over the width of the flange, as shown on fig. 2. Consequently, R is likewise distributed in this manner, instead of the uniform distribution shown on fig. 6a. In view of the approximate character of this calculation, and of the uncertainty as to the amount of edge restraint, the details of the actual distribution of s, and other factors, an elaborate modification of eq. 11 to account for the stress distribution of fig. 2 would represent a rather fictitious improvement. For this reason it is believed that a sufficiently close approximation is obtained, if, in eq. 11, the average stress of fig. 2 is substituted for s. From the definition of the equivalent width, this average stress is easily obtained from

$$s_{\rm av} = s_{\rm max} \left(\frac{b_c}{b} \right) \,. \tag{12}$$

For more information on this type of deformation, particularly for tension flanges, see the writer's earlier paper (4).

⁽⁴⁾ Geo. Winter, Stress-Distribution in, and Equivalent Width of Wide, Thin-Wall Steel Beams, Techn. Note No. 784. Advisory Comm. for Aeronautics, 1940, Washington, D. C.

In the tests reported herein, both types of deformation were clearly observed. That is, the flanges showed a general « dishing » (smooth downward deflection of the center line) on which was superposed the square-wave pattern of the buckling deformations. By means of special apparatus, the magnitude of these distortions of the flanges perpendicular to their original planes were measured at six points along the center line of each beam. It was found that at design loads (i.e. about $P_{yield}/1.85$) these deformations reached a maximum of 1 % of the flange width for two of the beams; and in most other cases they were closer to 1/2 %. Although these distortions are clearly visible, it can be said that their magnitude at design loads is sufficiently small so as not to interfere with the practical use of such light gage steel members.

In conclusion it should be said that the information given in this paper suffers from the evident disadvantage of being primarily empirical and approximate. The theoretical complexity of plate buckling at stresses larger than s_{cr} , as well as the large amount of possible variations of shape resulting in a wide range of conditions of edge restraint, precluded an analytical treatment of practical value. It is hoped that future investigations in this field, both mathematical and experimental, will elucidate some of the more detailed aspects of this problem.

NOTATION

b =flat width of flange.

 $b_{\epsilon} = \text{equivalent flange width.}$

c = distance from neutral axis to extreme fiber.

D = flexural plate rigidity.

 $=E t^3/12 (1-v^2)$.

 $M_b =$ bending moment in beam.

 $M_I =$ bending moment in flange.

 $r_b = \text{radius of curvature of beam.}$

 r_t = radius of curvature of flange.

s = stress in flange.

 s_{cr} = critical buckling stress of flange by small deflection theory.

 s_{yp} = yield stress of material.

t = flange thickness.

w =buckling deflection of flange.

x, y =coordinates. y =Poisson's ratio.

Résumé

L'emploi de profilés laminés normaux pour les petites portées et les charges relativement faibles n'est pas économique. Pour de telles constructions, les éléments en tôles minces laminées et pliées à froid ont fait leur preuve aux Etats-Unis. Des spécifications pour le calcul de constructions en tôles minces pliées furent publiées récemment, basées sur les recherches de l'auteur. Dans ce système, le comportement des ailes comprimées est d'une importance primordiale.

Pour de telles tôles, la tension de flambage calculée de la façon habituelle, ne représente pas la limite de la charge utile. Dans l'état de déformation, il y a une distribution irrégulière des tensions. On peut calculer le comportement de tels éléments constructifs en remplaçant la largeur réelle b par une largeur équivalente b_c , qui se calcule par une équation empirique. La limite de fluage devient la valeur critique des tensions calculées au moyen de b_c .

Une série d'essais caractéristiques a montré l'erreur moyenne très faible obtenue par le calcul de la charge utile, ainsi que la déformation, en se basant sur la largeur équivalente.

Une méthode approximative de calcul, amplement vérifiée par des mesures, est également indiquée pour la déformation des ailes dans l'état de déformation après flambage.

Zusammenfassung

Die Verwendung normaler Walzprofile ist bei kleineren Spannweiten und relativ leichter Belastung nicht wirtschaftlich. Für solche Bauwerke haben sich in den Vereinigten Staaten Elemente aus kalt gepressten oder gewalzten dünnen Blechen bewährt, für die auf Grund von Untersuchungen des Verfassers kürzlich Entwurfsvorschriften veröffentlicht wurden. In diesem Zusammenhang ist das Verhalten dünnwandiger Blech-Druckgurte von besonderer Bedeutung.

Für ein solches Blech stellt die auf die übliche Art berechnete Beulspannung nicht die Grenze der Tragfähigkeit dar. Im ausgebeulten Zustand tritt eine ungleichförmige Spannungsverteilung ein. Man kann das Verhalten solcher Bau-Elemente durch Ersetzen der wirklichen Breite b durch eine äquivalente Breite b_c berechnen, die sich mit Hilfe einer empirisch gefundenen Gleichung bestimmen lässt. Die Fliessgrenze wird für die auf Grund von b_c ermittelten Spannungen zum kritischen Wert.

Eine Reihe charakteristischer Versuche zeigte die nur geringen durchschnittlichen Fehler, die sich bei Berechnungen der Tragfähigkeit wie auch der Durchbiegungen auf Grund der äquivalenten Breite ergeben.

Ebenfalls wird für die Blechverformungen im ausgebeulten Zustand ein durch Messungen überprüftes angenähertes Berechnungsverfahren angegeben.

Summary

The use of conventional rolled steel shapes for small spans and comparatively light loads is uneconomical. For such constructions, light members, cold formed from sheet steel, have stood the test in the U. S. A. Specifications for the design of such members were recently issued, based on the author's investigations. In this connection, the performance of thin compression flanges is of particular importance.

For such plates the buckling stress calculated in the usual way does not represent the limit of carrying capacity. In the buckled state an irregular distribution of stresses occurs. The behaviour of such structural members can be calculated by replacing the actual width b by an equivalent width b_c , which can be ascertained with the help of an empirical equation. The yield point becomes the limiting value of the stresses as determined by means of b_c .

A series of characteristic tests showed only slight average errors arising from the calculations of the carrying capacity ,as well as deflection on the basis of the equivalent width.

An approximate method of calculation, amply proved by measurements, is also given for distortion of members in the buckled state.